Thermodynamic Studies of $[HPt(EtXantphos)_2]^+$ and $[(H)_2Pt(EtXantphos)_2]^{2+}$

Alex Miedaner,[†] James W. Raebiger,[†] Calvin J. Curtis,[†] Susie M. Miller,[§] and Daniel L. DuBois*[,†]

National Renewable Energy Laboratory, 1617 Cole Boulevard, Golden, Colorado 80401, and Department of Chemistry, Colorado State University, Fort Collins, Colorado 80523

Received October 15, 2003

$[HPt(EtXantphos)_2](PF_6)$ (where EtXantphos is 9,9-dimethyl-4,5-bis(diethylphosphino)-xanthene) can be prepared by the reduction of $Pt(COD)Cl_2$ (where COD is 1,4-cyclooctadiene) with hydrazine in the presence of 2 equiv of the diphosphine ligand followed by exchange of Cl^- with PF_6^-. Deprotonation of $[HPt(EtXantphos)_2](PF_6)$ ($pK_a = 27.3$ in acetonitrile) leads to the formation of $Pt(EtXantphos)_2$, which has been characterized by an X-ray diffraction study. $Pt(EtXantphos)_2$ has a distorted tetrahedral geometry. The average chelate bite angle is 108.2°, and the dihedral angle between the two planes formed by the phophorus atoms of each diphophine ligand and platinum is 80.4°. Protonation of $[HPt(EtXantphos)_2]^+$ results in the formation of $[(H)_2Pt(EtXantphos)_2]^{2+}$, which has a pK_a of 6.8 in acetonitrile. Oxidation of $Pt(EtXantphos)_2$ with ferrocenium tetrafluoroborate produces $[Pt(EtXantphos)_2]^{2+}$. $[Pt(EtXantphos)_2]^{2+}$ undergoes two reversible one-electron reductions ($E_{1/2}(II/I) = -0.81$ V versus ferrocene and $E_{1/2}(I/0) = -0.97$ V), and $[HPt(EtXantphos)_2]^+$ undergoes a reversible one-electron oxidation ($E_{1/2}(II/III) = +0.23$ V). These half-wave potentials and the pK_a values of $[HPt(EtXantphos)_2]^+$ and $[(H)_2Pt(EtXantphos)_2]^{2+}$ have been used to calculate five additional homolytic and heterolytic bond-dissociation free energies for these two hydride species and for $[HPt(EtXantphos)_2]^{2+}$. The extensive thermodynamic characterization of this hydride system provides useful insights into the factors controlling the reactivity of these complexes.

Introduction

The metal−hydrogen bond can be cleaved in three ways, as shown in Scheme 1. Perhaps the most extensively studied property of transition metal hydrides in solution is their acidity, shown as the reaction on the right of Scheme 1. This property of metal hydrides is determined by their pK_a values (a free-energy measurement) or their heats of protonation (an enthalpy measurement).[1−9] The homolytic cleavage of the metal−hydrogen bond, shown by the middle reaction in Scheme 1, results in the formation of the hydrogen atom and an associated metal fragment. The enthalpy associated with this reaction is the M−H bond energy, and it is this value that is typically associated with bond strengths.[10−12] The solution bond-dissociation free energy for the homolytic cleavage of an M−H bond can be calculated from the pK_a value of the metal hydride, the oxidation potential of the conjugate base of the metal hydride, and the reduction potential of the $(H^+/H^\bullet)$ couple using a thermodynamic cycle.[13] This method has been used to determine homolytic bond-dissociation free

Scheme 1

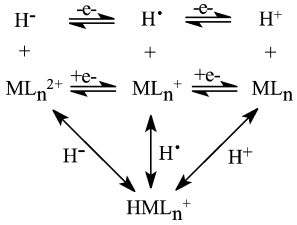

* To whom correspondence should be addressed. E-mail: dan_dubois@nrel.gov.
[†] National Renewable Energy Laboratory.
[§] Department of Chemistry, Colorado State University.

(1) Kristjánsdóttir, S. S.; Norton, J. R. *Transition Metal Hydrides*; Dedieu, A., Ed.; VCH: New York, 1991; pp 309−359.
(2) Jordan, R. F.; Norton, J. R. *J. Am. Chem. Soc.* **1982**, *104*, 1255−1263.
(3) Moore, E. J.; Sullivan, J. M.; Norton, J. R. *J. Am. Chem. Soc.* **1986**, *108*, 2257−2263.
(4) Kristjánsdóttir, S. S.; Moody, A. E.; Weberg, R. T.; Norton, J. R. *Organometallics* **1988**, *7*, 1983−1987.
(5) (a) Jessop, P. G.; Morris, R. H. *Coord. Chem. Rev.* **1992**, *121*, 155. (b) Abdur-Rashid, K.; Fong, T. P.; Greaves, B.; Gusev, D. G.; Hinman, J. G.; Landau, S. E.; Lough, A. J.; Morris, R. H. *J. Am. Chem. Soc.* **2000**, *122*, 9155−9171. (c) Morris, R. H. *Inorg. Chem.* **1992**, *31*, 1471−1478.
(6) Bullock, R. M.; Song, J.-S.; Szalda, D. J *Organometallics* **1996**, *15*, 2504−2516.
(7) Davies, S. C.; Henderson, R. A.; Hughes, D. L.; Oglieve, K. E. *J. Chem. Soc., Dalton Trans.* **1998**, 425−431.
(8) (a) Nataro, C.; Thomas, L. M.; Angelici, R. J. *Inorg. Chem.* **1997**, *36*, 6000−6008. (b) Nataro, C.; Angelici, R. J. *Inorg. Chem.* **1998**, *37*, 2975−2983. (c) Nataro, C.; Chen, J.; Angelici, R. J. *Inorg. Chem.* **1998**, *37*, 1868−1875. (d) Wang, D.; Angelici, R. J. *Inorg. Chem.* **1996**, *35*, 1321−1331. (e) Siclovan, O. P.; Angelici, R. J. *Inorg. Chem.* **1998**, *37*, 432−444.
(9) Pearson, R. G.; Kresge, C. T. *Inorg. Chem.* **1981**, *20*, 1878−1882.
(10) Simões, J. A. M.; Beauchamp, J. L. *Chem. Rev.* **1990**, *90*, 629−688.
(11) Kiss, G.; Zhang, K.; Mukerjee, S. L.; Hoff, C. D. *J. Am. Chem. Soc.* **1990**, *112*, 5657−5658.
(12) Schock, L. E.; Marks, T. J. *J. Am. Chem. Soc.* **1988**, *119*, 7701−7715.
(13) Wayner, D. M.; Parker, V. D. *Acc. Chem. Res.* **1993**, *26*, 287−294.

10.1021/om034238i CCC: $27.50
Publication on Web 04/21/2004

energies and enthalpies for a number of metal complexes, extending our knowledge of homolytic bond-dissociation energies.[13−17]

The thermodynamic hydride donor ability, or hydricity, of a metal hydride can be defined as the free energy associated with the heterolytic cleavage of the M−H bond to form solvated H^- and a solvated metal fragment. This reaction is shown on the left-hand side of Scheme 1. It is recognized that the ability of a transition metal hydride to act as a hydride donor is also an important property of these complexes. In fact, their name is derived from this property. A number of studies have addressed the issue of kinetic hydricity of metal hydrides,[18−23] but only recently have studies of the thermodynamic hydricities begun to appear.[24−32] If the metal complex resulting from deprotonation of a transition metal hydride can be oxidized reversibly by two electrons, then free energies for the heterolytic cleavage of the M−H bond to form H^- and the corresponding metal complex can be calculated using a simple thermodynamic cycle. This method has been used previously to determine the hydride donor abilities of a number of platinum hydrides of the type [HPt(diphosphine)$_2$]$^+$,[24] and the reliability of this method has been established by cross-checking these values with those obtained for the same complexes from the heterolytic cleavage of hydrogen.[26]

Studies of related nickel and palladium [HM(diphosphine)$_2$]$^+$ complexes have shown that the pK_a values of these complexes exhibit a linear dependence on the potentials of the Ni(I/0) and Pd(I/0) couples.[30,32] Similarly, the hydricities of these complexes depend on the potentials of the Ni(II/I) and Pd(II/I) couples. However, it was not possible to establish similar free-energy relationships for [HPt(diphosphine)$_2$]$^+$ complexes with small chelate bite angles, because oxidation of the corresponding Pt(0) complexes occurs by two-electron processes. Previous work from our laboratory has demonstrated that diphosphine ligands with large bite angles can be used to stabilize the d^9 electronic configuration, that is Ni(I) and Pd(I) complexes.[32,33] Longato and co-workers have obtained similar results for Ir(0) complexes, which are also 17-electron d^9 complexes.[34] In this paper, we report the use of the EtXantphos ligand to resolve the two-electron oxidation processes that are typically observed for Pt(diphosphine)$_2$ complexes into two one-electron processes. Because the potentials of both the Pt(II/I) and Pt(I/0) couples can be measured, all three bond-dissociation free energies can be determined for [HPt(Xantphos)$_2$]$^+$. In addition, [HPt(Xantphos)$_2$]$^+$ undergoes a reversible one-electron oxidation and a reversible protonation. These features allow the homolytic bond-dissociation free energies and pK_a values of [(H)$_2$Pt(EtXantphos)$_2$]$^{2+}$ and [HPt(EtXantphos)$_2$]$^{2+}$ to be calculated. As a result, a much more comprehensive thermodynamic characterization of the Pt−H bond has been obtained than was possible in previous studies.

Experimental Section

Syntheses. All manipulations were performed under an inert atmosphere using standard Schlenk techniques or a glovebox. Solvents were distilled under nitrogen using standard procedures. Ni(dmpe)$_2$ (where dmpe is bis(dimethylphosphino)ethane),[24] EtXantphos (9,9-dimethyl-4,5-bis(diethylphosphino)xanthene),[32,35] and $(Me_2N)_3P{=}NMe$[36] were prepared using literature methods. The acid [$(Me_2N)_3P{=}NHMe$](BF$_4$) (pK_a = 27.5)[36] was prepared by reacting $(Me_2N)_3P{=}NMe$ in ether with HBF$_4$·OMe$_2$ and isolating the off-white precipitate. Cyanoanilinium tetrafluoroborate was prepared by reacting 4-cyanoaniline with HBF$_4$·OMe$_2$ in ether and washing the resulting solid with ether.

[HPt(EtXantphos)$_2$](PF$_6$), 1. A mixture of Pt(COD)Cl$_2$ (0.38 g, 1.0 mmol) and EtXantphos (0.78 g, 2.0 mmol) in acetonitrile (50 mL) was stirred at room temperature for 1 h (a ^{31}P NMR spectrum showed a complex mixture at this point), and then hydrazine (0.5 mL, 16 mmol) was added to this solution. The mixture was stirred overnight to form a clear yellow solution. Reducing the volume to 10 mL and adding diethyl ether (50 mL) resulted in a yellow powder (0.90 g, 90%). This solid was dissolved in dichloromethane (50 mL), and a solution of ammonium hexafluorophosphate (2.9 g, 20 mmol) in water (50 mL) was added. After vigorously stirring the resulting mixture for 3 h, the organic phase was separated,

(14) (a) Tilset, M.; Parker, V. D. *J. Am. Chem. Soc.* **1989**, *111*, 6711−6717. (b) Tilset, M.; Parker, V. D. *J. Am. Chem. Soc.* **1990**, *112*, 2843.
(15) Parker, V. D.; Handoo, K. L.; Roness, F.; Tilset, M. *J. Am. Chem. Soc.* **1991**, *113*, 7493−7498.
(16) Ryan, B. O.; Tilset, M.; Parker, V. D *J. Am. Chem. Soc.* **1990**, *112*, 2618−2626.
(17) Wang, D.; Angelici, R. J. *J. Am. Chem. Soc.* **1996**, *118*, 935−942.
(18) (a) Labinger, J. A. In *Transition Metal Hydrides*; Dedieu, A., Ed.; VCH: New York, 1991; pp 361−379. (b) Labinger, J. A.; Komadina, K. H. *J. Organomet. Chem.* **1978**, *155*, C25−C28.
(19) (a) Kao, S. C.; Spillett, C. T.; Ash, C.; Lusk, R.; Park, Y. K.; Darensbourg, M. Y. *Organometallics* **1985**, *4*, 83−91. (b) Kao, S. C.; Gaus, P. L.; Youngdahl, K.; Darensbourg, M. Y. *Organometallics* **1984**, *3*, 1601−1603. (c) Gaus, P. L.; Kao, S. C.; Youngdahl, K.; Darensbourg, M. Y. *J. Am. Chem. Soc.* **1985**, *107*, 2428−2434. (d) Kinney, R. J.; Jones, W. D.; Bergman, R. G. *J. Am. Chem. Soc.* **1978**, *100*, 7902−7915.
(20) Martin, B. D.; Warner, K. E.; Norton, J. R. *J. Am. Chem. Soc.* **1986**, *108*, 33−39.
(21) Cheng, T.-Y.; Bullock, R. M. *J. Am. Chem. Soc.* **1999**, *121*, 3150−3155. (b) Cheng, T.-Y.; Brunschwig, B. S.; Bullock, R. M. *J. Am. Chem. Soc.* **1998**, *120*, 13121−13137. (c) Bullock, R. M.; Voges, M. H. *J. Am. Chem. Soc.* **2000**, *122*, 12594−12595. (d) Cheng, T.-Y.; Bullock, R. M. *Organometallics* **2002**, *21*, 2325−2331. (e) Song, J.-S.; Szalda, D. J.; Bullock, R. M. *Organometallics* **2001**, *20*, 3337−3346.
(22) Kobayashi, A.; Takatori, R.; Kikuchi, I.; Konno, H.; Sakamoto, K.; Ishitani, O. *Organometallics* **2001**, *20*, 3361−3363.
(23) Xu, A. N.; Studebaker, D. B.; Westmoreland, T. D. *Organometallics* **1996**, *15*, 4888−4890.
(24) Berning, D. E.; Noll, B. C.; DuBois, D. L. *J. Am. Chem. Soc.* **1999**, *121*, 11432−11447.
(25) Ellis, W. W.; Miedaner, A.; Curtis, C. J.; Gibson, D. H.; DuBois, D. L. *J. Am. Chem. Soc.* **2002**, *124*, 1926−1932.
(26) Curtis, C. J.; Miedaner, A.; Ellis, W. W.; DuBois, D. L. *J. Am. Chem. Soc.* **2002**, *124*, 1918−1925.
(27) (a) Sarker, N.; Bruno, J. W. *J. Am. Chem. Soc.* **1999**, *121*, 2174−2180. (b) Sarker, N.; Bruno, J. W. *Organometallics* **2001**, *20*, 55−61.
(28) Ciancanelli, R. F.; Noll, B. C.; DuBois, D. L.; DuBois, M. R. *J. Am. Chem. Soc.* **2002**, *124*, 2984−2992.
(29) Price, A. J.; Ciancanelli, R.; Noll, B. C.; Curtis, C. J.; DuBois,D. L.; DuBois, M. R. *Organometallics* **2002**, *21*, 4833−4839.
(30) Berning, D. E.; Miedaner, A.; Curtis, C. J.; Noll, B. C.; DuBois, M. R.; DuBois, D. L. *Organometallics* **2001**, *20*, 1832−1839.
(31) Ellis, W. W.; Ciancanelli, R.; Miller, S. M.; Raebiger, J. W.; DuBois, M. R.; DuBois, D. L. *J. Am. Chem. Soc.* **2003**, *125*, 12230−12236.
(32) Raebiger, J. W.; Miedaner, A.; Curtis, C. J.; Miller, S. M.; DuBois, D. L. *J. Am. Chem. Soc.* **2004**, *126*, accepted.
(33) (a) Miedaner, A.; Haltiwanger, R. C.; DuBois, D. L. *Inorg. Chem.* **1991**, *30*, 417−427. (b) Wander, S. A.; Miedaner, A.; Noll, B. C.; DuBois, D. L. *Organometallics* **1996**, *15*, 3360.
(34) Longato, B.; Riello, L.; Bandoli, G. Pilloni, G. *Inorg. Chem.* **1999**, *38*, 2818−2823.
(35) Kranenburg, M.; van der Burgt, Y. E. M.; Kamer, P. C. J.; van Leewen, P. W. N. M.; Goubitz, K.; Fraanje, J. *Organometallics* **1995**, *14*, 3081−3089.
(36) (a) Schwesinger, R.; Schlemper, H. *Angew. Chem., Int. Ed. Engl.* **1987**, *26*, 1167−1169. (b) Appel, R.; Halstenberg, M. *Angew. Chem., Int. Ed. Engl.* **1977**, *16*, 263−264.

washed with water (5 × 25 mL) to remove ammonium chloride, and dried over molecular sieves. Removal of the solvent with a vacuum and recrystallization of the resulting solid from acetonitrile/toluene (1:10) yielded 0.51 g (51%) of product. ^{1}H NMR (CD_3CN): δ 7.60 (d, 4 H, J = 8 Hz, Ar-*H*); 7.37 (br s, 2 H, Ar-*H*); 7.30 (br s, 2 H, Ar-*H*); 7.19 (br s, 2 H, Ar-*H*); 6.27 (br s, 2 H, 2,7-H); 2.43 (br m, 4 H, PCH_2CH_3); 2.15 (br m, 4 H, PCH_2CH_3); 2.04 (br m, 2 H, PCH_2CH_3); 1.88 (br s, 6 H, 9-CH_3); 1.36 (br s, 6 H, 9-CH_3); 1.31 (br s, 6 H, PCH_2CH_3); 0.92 (br s, 8 H, PCH_2CH_3 and PCH_2CH_3); 0.62 (br s, 8 H, PCH_2CH_3 and PCH_2CH_3); −0.09 (br s, 6 H, PCH_2CH_3); −0.60 (br, 2 H, PCH_2CH_3); −15.00 (br t of t, $^2J_{PH}$ = 80 Hz, $^2J_{PH}$ = 15 Hz, $^1J_{PtH}$ = 534 Hz). ^{31}P NMR (CD_3CN): δ −24.89 (t, $^2J_{PP}$ = 65 Hz, $^1J_{PtP}$ = 2836 Hz); −29.13 (br m, $^1J_{PtP}$ = 2340 Hz). IR (Nujol mull): ν_{PtH} 2175 and 2197 cm^{-1}. IR (CH_2Cl_2): ν_{PtH} 2147 and 2188 cm^{-1}. Anal. Calcd for $C_{46}H_{65}F_6O_2P_5Pt$: C, 49.60; H, 5.88; P, 13.90. Found: C, 49.67; H, 5.92; P, 13.79.

Pt(EtXantphos)$_2$, 2. A solution of [HPt(EtXantphos)$_2$]Cl (0.96 g, 0.96 mmol) in acetonitrile (50 mL) was treated with solid potassium *tert*-butoxide (0.107 g, 0.96 mmol). The mixture was stirred overnight, the solvent was removed under vacuum, and the resulting yellow solid was dissolved in toluene (50 mL). Insoluble products were removed by filtration, and the volume of the filtered solution was reduced to about 2 mL. Addition of acetonitrile (2 mL) resulted in formation of an orange microcrystalline product (0.56 g, 61%), which was isolated by filtration and dried in a vacuum. ^{1}H NMR (toluene-d_8): δ 7.16 (br s, 4 H, Ar-*H*), 7.14 (br s, 4 H, Ar-*H*) and 6.52 (br s, 2 H, Ar-*H*); 2.50, 1.86, −0.66 (2 H) (br m's, PCH_2CH_3); 1.39, 1.04, 0.63, −0.22 (br m's, PCH_2CH_3); 1.65 and 1.39 (br s, 9-CH_3). ^{1}H NMR at −40 °C (toluene-d_8): δ 6.59 (d, J = 6 Hz, 2 H, Ar−H); 2.60 (br m, 4 H, PCH_2CH_3); 2.53 (br m, 2 H, PCH_2CH_3); 1.87 (m, 4 H, PCH_2CH_3); 1.24 (br m, 2 H, PCH_2CH_3); 1.05 (br m, 2 H, PCH_2CH_3); −0.82 (m, 2 H, PCH_2CH_3); 1.38 (m, 6 H, PCH_2CH_3); 1.10 (m, 6 H, PCH_2CH_3); 0.65 (m, 6 H, PCH_2CH_3); −0.26 (p, J = 7 Hz, 6 H, PCH_2CH_3); 1.62 (s, 7 H, 9-CH_3); and 1.44 (s, 7 H, 9-CH_3). ^{31}P NMR (toluene-d_8): δ −6.82 (t, $^2J_{PP}$ = 48 Hz, $^1J_{PtP}$ = 4086 Hz); −19.65 (t, $^1J_{PtP}$ = 3602 Hz). Anal. Calcd for $C_{46}H_{64}O_2P_4Pt$: C, 57.08; H, 6.66; P, 12.80. Found: C, 57.08; H, 6.60; P, 12.68.

[Pt(EtXantphos)$_2$](BF$_4$)$_2$, 3. A solution of Pt(EtXantphos)$_2$ (0.20 g, 0.21 mmol) in toluene (30 mL) was treated with ferrocenium tetrafluoroborate (0.12 g, 0.42 mmol) in acetonitrile (10 mL). The resulting dark yellow solution was stirred at room temperature for 2 h. Removing the solvent with a vacuum yielded a yellow powder, which was washed with hexanes (three 10-mL aliquots). Recrystallization from acetonitrile/diethyl ether (1:5) gave a yellow microcrystalline product (0.15 g, 64%), which was isolated by filtration and dried under a vacuum. ^{1}H NMR (CD_3CN): δ 7.82 (br d, $^3J_{HH}$ = 8 Hz, 4 H, 1,8-H); 7.48 (t, 4 H, 2,7-H); 7.38 (br m, 4 H, 3,6-H); 2.3−1.8 (br m's, 15 H, PCH_2CH_3); 1.67 (br s, 12 H, 9-CH_3); 0.77 (br m, 24 H, PCH_2CH_3). ^{31}P NMR (CD_3CN): δ 2.09 (br s, $^1J_{PtP}$ = 2601 Hz). Anal. Calcd for $C_{46}H_{64}B_2F_8O_2P_4Pt$: C, 48.40; H, 5.65; P, 10.85. Found: C, 48.34; H, 5.52; P, 10.67.

Reaction of [Pt(EtXantphos)$_2$](BF$_4$)$_2$ with H$_2$ in Acetonitrile-d_3 and Dimethylformamide-d_7. In a typical experiment, [Pt(EtXantphos)$_2$](BF$_4$)$_2$ (approximately 20 mg) was dissolved in CD_3CN (0.6 mL) in an NMR tube. The resulting solution was purged with H_2 for 15 min and placed on a shaker. The samples were monitored daily by ^{1}H and ^{31}P NMR spectroscopy for 1 week. After 4 days, [Pd(EtXantphos)$_2$](BF$_4$)$_2$ was no longer observed and resonances corresponding to [HPt(EtXantphos)$_2$](BF$_4$) and [(H)$_2$Pt(EtXantphos)$_2$](BF$_4$)$_2$, **4**, were observed in a nearly 1:1 ratio. Similar experiments were repeated using DMF-d_7 as the solvent. In this case, [HPt(EtXantphos)$_2$](BF$_4$) is the only product observed, and the reaction reaches completion in approximately 4 days. ^{1}H NMR for [(H)$_2$Pt(EtXantphos)$_2$](BF$_4$)$_2$, **4** (CD_3CN): δ 8.53 (br m, Ar-*H*); 8.04 (d, $^3J_{HH}$ = 7 Hz, Ar-*H*); 7.87 (d, $^3J_{HH}$ = 8 Hz, Ar-*H*); 7.73 (d, $^3J_{HH}$ = 7 Hz, Ar-*H*); 7.61 (d, $^3J_{HH}$ = 8 Hz, Ar-*H*); 7.5−7.4 (br m's, Ar-*H*); 7.20 (t, $^3J_{HH}$ = 7 Hz, Ar-*H*); 7.04 (br m, Ar-*H*); 6.79 (t, $^3J_{HH}$ = 7 Hz, Ar-*H*); 2.75 (br s, PCH_2CH_3 or PCH_2CH_3); 2.41 (br m, PCH_2CH_3 or PCH_2CH_3); 2.22 (br s, PCH_2CH_3 or PCH_2CH_3); 1.72 (s, 9,10-CH_3); 1.63 (br s, PCH_2CH_3 or PCH_2CH_3); 1.26 (br s, PCH_2CH_3 or PCH_2CH_3) 1.14 (dt, $^3J_{PH}$ = 21 Hz, $^3J_{HH}$ = 7 Hz, PCH_2CH_3); 0.73 (br m, PCH_2CH_3 or PCH_2CH_3); 0.33 (br s, PCH_2CH_3 or PCH_2CH_3); −8.1 (d of t of d with Pt satellites; $^2J_{AX}$ = 163 Hz, $^2J_{AX'}$ = 6 Hz, $^2J_{BX}$ = 17 Hz, $^1J_{HPt}$ = 812 Hz; see Figure 2). ^{31}P NMR (CD_3CN): This spectrum is broad and complex with major resonances at δ = 12.83, 9.40, 6.53, 4.85, 4.07, 3.43, 3.30, 2.75, and −3.08.

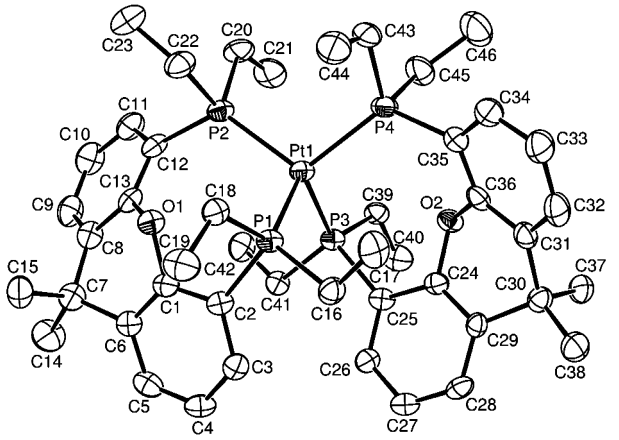

Figure 1. Drawing of Pt(EtXantphos)$_2$ showing atom-numbering scheme and thermal ellipsoids.

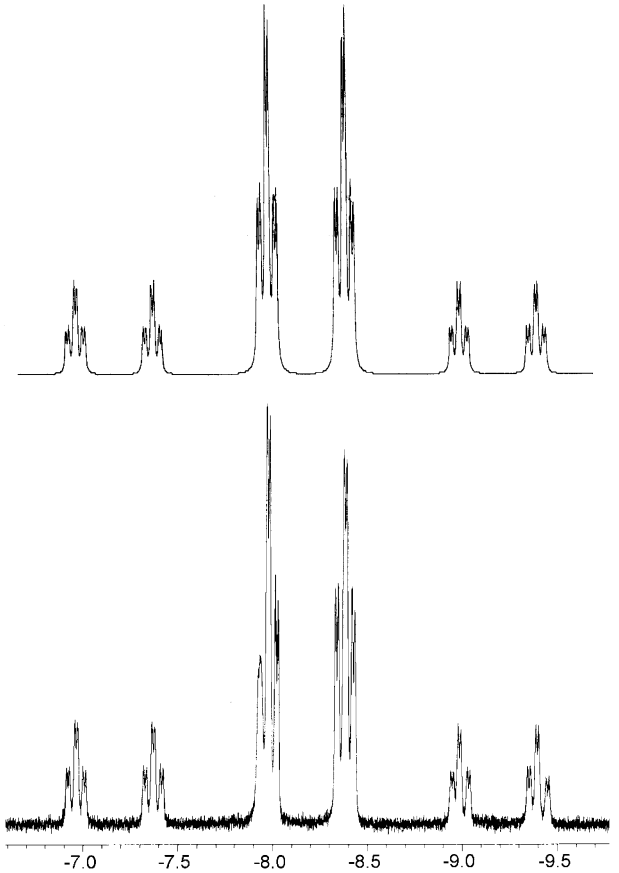

Figure 2. ^{1}H NMR of the hydride region of [(H)$_2$Pt(EtXantphos)$_2$]$^{2+}$. The bottom trace is an experimental spectrum. The top trace is a simulated spectrum using parameters given in the text.

Physical Measurements. NMR spectra were recorded on a Varian Inova 400 MHz spectrometer. ^{1}H chemical shifts

are reported relative to tetramethylsilane using residual solvent protons as a secondary reference. ^{31}P chemical shifts are reported relative to external phosphoric acid, and all ^{31}P NMR spectra were proton decoupled. All electrochemical measurements were carried out under an N_2 atmosphere in 0.3 M Et_4NBF_4 in acetonitrile or in 0.2 M Bu_4NBF_4 in benzonitrile or dichloromethane. Cyclic voltammetry experiments were carried out on a Cypress Systems computer-aided electrolysis system. The working electrode was a glassy carbon disk (2 mm diameter), and the counter electrode was a glassy carbon rod. A platinum wire immersed in a permethylferrocene/permethylferrocenium solution was used to fix the potential. Ferrocene was used as an internal standard, and all potentials are referenced to the ferrocene/ferrocenium couple.

pK_a of [(H)$_2$Pt(EtXantphos)$_2$]$^{2+}$. In a typical experiment, [HPt(EtXantphos)$_2$](PF$_6$) (11 mg, 0.01 mmol) and cyanoanilinium tetrafluoroborate (pK_a = 7.6)[37] (41 mg, 0.20 mmol) were accurately weighed into an NMR tube and dissolved in benzonitrile (0.6 mL). A known quantity of 4-cyanoaniline (7 mg, 0.06 mmol) was added via a gastight syringe. The solution was mixed and monitored by ^{1}H NMR (hydride region only) and ^{31}P NMR (unlocked). The reaction came to equilibrium within 20 min and was monitored every several hours for 24 h to ensure that the ratios had not changed. The ^{1}H and ^{31}P NMR resonances assigned to [(H)$_2$Pt(EtXantphos)$_2$]$^{2+}$ and [HPt(EtXantphos)$_2$]$^+$ were integrated, and the ratio was used to determine the equilibrium constant for the reaction. The same values were obtained from both the ^{31}P and ^{1}H NMR spectra. Four separate experiments were run to determine the reproducibility. The equilibrium constant of 0.14 ± 0.03 was used to calculate a pK_a of 6.8 for [(H)$_2$Pt(diphosphine)$_2$]$^{2+}$. Similar experiments carried out using excess triflic acid and tetrafluoroboric acid also resulted in the formation of [(H)$_2$Pt(EtXantphos)$_2$]$^{2+}$ based on ^{1}H NMR and ^{31}P NMR spectra.

pK_a of [HPt(EtXantphos)$_2$]$^+$. Method A. In a typical experiment, [HPt(EtXantphos)$_2$](PF$_6$) (11 mg, 0.01 mmol) and Ni(dmpe)$_2$ (18 mg, 0.05 mmol) were disolved in benzonitrile (0.6 mL). The reaction was monitored for 8 h by ^{31}P NMR and ^{1}H NMR (hydride region only) spectroscopy. Integrations of ^{1}H and ^{31}P NMR spectra recorded between 3 and 8 h for four separate experiments were used to determine an equilibrium constant of (1.0 ± 0.4) × 10^{-3}. A pK_a value of 27.3 for [HPt(EtXantphos)$_2$](PF$_6$) was calculated from these data and the pK_a of [HNi(dmpe)$_2$]$^+$ (24.3).[24]

Method B. [(Me$_2$N)$_3$P=NHMe](BF$_4$) (4 mg, 0.014 mmol, pK_a = 27.5[36]) was dissolved in 0.7 mL of PhCN and added to Pt(EtXantphos)$_2$ (14 mg, 0.014 mmol) in an NMR tube. The homogeneous orange solution was shaken and monitored by ^{31}P NMR over a period of several days. The reaction came to equilibrium in 5 days. An equilibrium constant of 0.51 was determined by integration of the ^{31}P NMR spectrum. The pK_a of [HPt(EtXantphos)$_2$]$^+$ was calculated to be 27.2 using these data.

X-ray Crystallography. X-ray diffraction data for a selected crystal of Pt(EtXantphos)$_2$ were recorded on a Bruker Nonius SMART CCD diffractometer employing Mo Kα radiation (graphite monochromator). Selected details related to the crystallographic experiment for Pt(EtXantphos)$_2$ are listed in Table 1. Unit cell parameters were obtained from a least-squares fit to the angular coordinates of all reflections, and intensities were integrated from a series of frames (0.3° ω rotation) covering more than a hemisphere of reciprocal space. Absorption and other corrections were applied by using SADABS.[38] The structure was solved by using direct methods and refined (on F^2, using all data) by a full-matrix, weighted least-squares process. All non-hydrogen atoms were refined by using anisotropic displacement parameters. Hydrogen atoms were placed in idealized positions and refined by using a riding model. Standard Bruker Nonius control (SMART) and integration (SAINT) software was employed, and Bruker Nonius SHELXTL[39] software was used for structure solution and refinement. Thermal ellipsoid plots were generated with the program ORTEP-3 for Windows.[40]

Table 1. Crystalographic Data and Structure Refinement for Pt(EtXantphos)$_2$

empirical formula	$C_{46}H_{64}O_2P_4Pt$
fw	967.94
temperature	173(2) K
wavelength	0.71073 Å
cryst syst	triclinic
space group	$P\bar{1}$
unit cell dimens	a = 11.077(3) Å, α = 90.549(5)°
	b = 14.132(4) Å, β = 109.599(4)°
	c = 15.845(5) Å, γ = 106.104(5)°
volume	2230.4(11) Å^3
Z	2
density(calcd)	1.441 g/cm^3
absorp coeff	3.324 mm^{-1}
F(000)	988
cryst size	0.40 × 0.40 × 0.20 mm^3
θ range for data collection	2.02−23.29°
index ranges	$-12 \le h \le 12$, $-15 \le k \le 15$,
	$-17 \le l \le 17$
no. of reflns collected	13 825
no. of indep reflns	6360 [R(int) = 0.0509]
completeness to θ = 23.29°	98.6%
absorp corr	SADABS
refinement method	full-matrix least-squares on F^2
no. of data/restraints/params	6360/0/479
goodness-of-fit on F^2	1.002
final R indices [$I > 2\sigma(I)$]	R1 = 0.0400, wR2 = 0.0936
R indices (all data)	R1 = 0.0480, wR2 = 0.0967
extinction coeff	0.0081(4)
largest diff peak and hole	2.092 and −1.456 e Å^{-3}
	(near Pt1 1.2 Å)

Results

Synthesis and Characterization of Metal Complexes. [HPt(EtXantphos)$_2$](PF$_6$), **1**, can be prepared by reaction of 2 equiv of EtXantphos with Pt(COD)Cl$_2$ followed by reduction with excess hydrazine and metathesis of the chloride salt with ammonium hexafluorophosphate (reaction 1). At room temperature, the ^{1}H NMR spectrum of [HPt(EtXantphos)$_2$](PF$_6$) exhibits the resonances expected for the presence of the EtXantphos ligand (see Experimental Section), and the hydride resonance appears as a broad triplet of triplets at −14.9 ppm with ^{195}Pt satellites. The ^{31}P NMR spectrum consists of two broad triplets at −29.3 and −25.2 ppm with ^{195}Pt satellites. At 80 °C, the ^{31}P NMR spectrum is a single broad resonance consistent with four equivalent phosphorus atoms, and a broad quintet with ^{195}Pt satellites is observed at −15.1 ppm in the hydride region of the ^{1}H NMR spectrum. The infrared spectrum (Nujol mull) exhibits two bands at 2197 and 2175 cm^{-1} assigned to Pt−H stretching modes. The infrared spectrum recorded in dichloromethane at room temperature also exhibits two bands at 2188 and 2147 cm^{-1}. This indicates that the origin of the two bands is not a solid state effect.

These spectral data are consistent with structure **1** and two dynamic processes. One dynamic process is

(37) Edidin, R. T.; Sullivan, J. M.; Norton, J. R. *J. Am. Chem. Soc.* **1987**, *109*, 3945−3953.
(38) Sheldrick, G. M. *SADABS, a program for area detector absorption corrections*.
(39) Sheldrick, G, M. *SHELXTL*, v. 6.12; Bruker AXS: Madison, WI, 1999.
(40) Farrugia, L. J. *J. Appl. Crystallogr.* **1997**, *30*, 565.

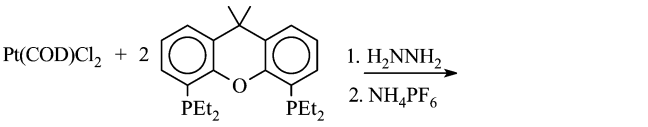

EtXantphos (1)

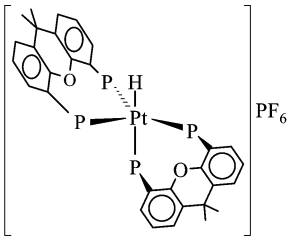

1

hydride migration from one face of a distorted tetrahedron to another, which occurs at all temperatures studied, and the other dynamic process is the inversion of the ring conformation of the bidentate EtXantphos ligands. Structure **1** can be regarded as a distorted trigonal bipyramid or a face-capped tetrahedron. This structure is the most common one observed for 18-electron $[HMP_4]^+$ complexes.[28,41] If the hydride ligand is fluxional and moves from one face of a tetrahedron to another, it will encounter two environments. In one environment the backbone of the EtXantphos ligand is folded toward the hydride ligand as shown in structure **1**, and in the other environment the backbone is folded away from the hydride ligand. On the IR time scale these two environments are distinguishable, and as a result, two IR bands are observed. On the slower time scale of the ^{1}H NMR experiment, these two environments are averaged by hydride migration from one face to the other. Only one resonance is observed for the hydride ligand over the entire temperature range studied (−40 to +80 °C), although the appearance of this resonance changes from a triplet of triplets at room temperature and below to a quintet at 80 °C.

The observation that the ^{31}P NMR spectrum is temperature dependent suggests a dynamic process for the phosphorus nuclei as well. As a result of the rapid hydride migration, the average environment of the four phosphorus atoms is best described as a distorted tetrahedron. As discussed in the next paragraph, Pt(EtXantphos)$_2$ is also a distorted tetrahedron, and the backbone of the bidentate EtXantphos ligand folds toward two faces of the tetrahedron and away from the other two. As a result, there are two different pairs of faces of the tetrahedron and two nonequivalent pairs of phosphorus atoms. A similar argument holds for the PtP_4 core of $[HPt(EtXantphos)_2]^+$. A rapid inversion of the ligand conformation would result in the two faces of the PtP_4 tetrahedral core of $[HPt(EtXantphos)_2]^+$ becoming equivalent, which is consistent with the observation of a single broad resonance in the ^{31}P NMR spectrum at 80 °C. The resonance for the hydride ligand also changes from a broad triplet of triplets with ^{195}Pt satellites at room temperature and below to a quintet with ^{195}Pt satellites at high temperature (80 °C). This is also consistent with the four phosphorus atoms becoming equivalent. In summary, the IR data suggest that the hydride ligand resides on both pairs of faces of a capped tetrahedron. The spectral characteristics of the hydride region of the ^{1}H NMR spectrum and the ^{31}P NMR spectra indicate that the hydride ligand moves between the two pairs of tetrahedral faces rapidly on the ^{1}H NMR time scale between −40 and +80 °C. A slower process that involves the inversion of the conformation of the ring formed by the EtXantphos ligand and Pt results in the phosphorus atoms becoming equivalent at 80 °C and above.

Table 2. Selected Bond Distances (Å) and Bond Angles (deg) for Pt(EtXantphos)$_2$

Bond Distances	
Pt(1)−P(2)	2.2893(18)
Pt(1)−P(4)	2.2915(18)
Pt(1)−P(3)	2.3119(17)
Pt(1)−P(1)	2.3124(17)
Bond Angles	
P(2)−Pt(1)−P(4)	107.77(6)
P(2)−Pt(1)−P(3)	117.04(6)
P(4)−Pt(1)−P(3)	108.44(6)
P(2)−Pt(1)−P(1)	108.07(6)
P(4)−Pt(1)−P(1)	116.24(7)
P(3)−Pt(1)−P(1)	99.50(6)

Deprotonation of $[HPt(EtXantphos)_2]^+$ with potassium *tert*-butoxide in acetonitrile results in the formation of Pt(EtXantphos)$_2$, **2**. Crystals of this compound can be grown from acetonitrile, and a structural study of this complex has been completed. Table 1 lists crystallographic data and some solution and refinement details. Table 2 lists selected bond distances and bond angles. Figure 1 shows a perspective drawing of the Pt(EtXantphos)$_2$ molecule. The overall geometry of this complex is a slightly distorted tetrahedron. The angle between the two phosphorus atoms on the same diphosphine ligand is 108.2°, and the remaining four angles range from 99.5° for the P(3)−Pt(1)−P(1) angle to 117.0° for the P(2)−Pt(1)−P(3) angle. The dihedral angle between the two planes formed by Pt and the two phosphorus atoms of each EtXantphos ligand is 80.4°, close to the expected 90° for a tetrahedron. The average Pt−P bond distance (2.30 Å) is slightly longer than that observed for Pt(dmpp)$_2$ (2.27 Å).[24]

From Figure 1, it can be seen that the xanthene backbone of the P(1)−P(2) ligand is folded toward P(3) and away from P(4). Similarly, the xanthene ring of the P(3)−P(4) ligand is folded toward P(1) and away from P(2). As a result, there are two pairs of phosphorus atoms. This is reflected in the ^{31}P NMR spectrum from room temperature to −40 °C in acetonitrile. Two triplet resonances are observed at −6.82 and −19.65 ppm at room temperature. Warming the NMR sample results first in a coalescence of these resonances and then in a single broad resonance at −13.4 ppm at 80 °C in the ^{31}P NMR spectrum. These spectral changes are fully reversible, and the original spectrum is observed upon returning to room temperature. It can be seen in Figure 1 that C(41) and C(16) are in close proximity to the arene rings C(1)−C(6) and C(24)−C(29), respectively. This interaction results in an unusual upfield shift of the methylene resonance (−0.66 ppm) in the ^{1}H NMR spectrum. A similar interaction is seen between the aromatic hydrogen atoms on C(3) and C(26) and the C(24)−C(29) and C(1)−C(6) arene rings. This also

(41) (a) Aresta, M.; Dibenedetto, A.; Amodio, E.; Papai, I.; Schubert, G. *Inorg. Chem*. **2002**, *41*, 6550−6552. (b) Miedaner, A.; DuBois, D. L.; Curtis, C. J.; Haltiwanger, R. C. *Organometallics* **1993**, *12*, 299−303.

Scheme 2

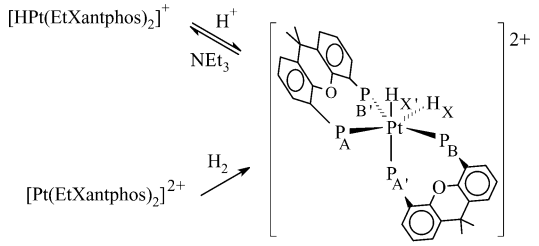

4

produces a significant upfield shift of this resonance from 7.22 ppm in the free ligand to 6.52 ppm in the metal complex.

Oxidation of Pt(EtXantphos)$_2$ with 2 equiv of ferrocenium tetrafluoroborate produces [Pt(EtXantphos)$_2$](BF$_4$)$_2$, **3**. The ^{31}P NMR spectrum of this product at −95 °C is a broad AB quartet (with ^{195}Pt satellites) centered at 2.00 ppm with $N = 334$ Hz. This pattern is consistent with an AA′BB′ spin system. The structure of [Pt(EtXantphos)$_2$]$^{2+}$ is expected to be a tetrahedrally distorted square-planar complex. For the analogous [Pd(EtXantphos)$_2$]$^{2+}$complex, the chelate bite angle is 139.7°, and the dihedral angle between the two diphosphine ligands is 89.0°.[32] In this case, the bidentate ligand spans the two trans positions of the square-planar complex, and the nonequivalence of the phosphorus atoms is a consequence of the eight-membered ring folding toward one phosphorus atom and away from the other phosphorus atom of the second EtXantphos ligand. It seems reasonable that the same structural features may be present in [Pt(EtXantphos)$_2$]$^{2+}$. This is supported by a very similar ^{31}P NMR spectrum for [Pd(EtXantphos)$_2$]$^{2+}$ at −40 °C, i.e., an AB quartet with $N = 348$ Hz.

Protonation of [HPt(EtXantphos)$_2$]$^+$ with triflic acid in acetonitrile-d_3, benzonitrile, or dichloromethane-d_2 results in the formation of [(H)$_2$Pt(EtXantphos)$_2$]$^{2+}$, **4**, as shown in the top reaction of Scheme 2. This reaction is reversible. When the solution is treated with excess triethylamine, [HPt(EtXantphos)$_2$]$^+$ is re-formed. [(H)$_2$Pt(EtXantphos)$_2$]$^{2+}$ is also formed when a deuterioacetonitrile solution of [Pt(EtXantphos)$_2$]$^{2+}$ is reacted with hydrogen (bottom reaction in Scheme 2). In deuterioacetonitrile, the monohydride complex, **1**, forms after [(H)$_2$Pt(EtXantphos)$_2$]$^{2+}$ formation due to basic impurities in the solvent or NMR tube. In deuterated dimethylformamide, which is more basic and better at solvating protons than acetonitrile, only the monohyride is formed under H_2.

The hydride region of the ^{1}H NMR spectrum of [(H)$_2$Pt(EtXantphos)$_2$]$^{2+}$ in deuterioacetonitrile is shown by the bottom trace in Figure 2. The top trace is a simulated spectrum. The hydride resonance is a doublet of a triplet of doublets, which is characteristic of octahedral *cis*-dihydrides. It can be analyzed in the following manner. The large doublet splitting arises from the coupling of each hydride, X and X′ of structure **4**, to the corresponding trans phosphorus atom, A and A′, respectively ($^2J_{AX} = {}^2J_{A'X'} = 163$ Hz). The triplet results from coupling of each hydride, X and X′, to the two phosphorus atoms, B and B′, that are cis to the hydride ligands ($^2J_{BX} = {}^2J_{B'X} = {}^2J_{BX'} = {}^2J_{B'X'} = 17$ Hz). Finally, the small doublet splitting is caused by coupling of each hydride, X and X′, to the cis phophorus atom, A′ and A, respectively ($^2J_{AX'} = {}^2J_{A'X} = 6$ Hz). The expected Pt satellites are also observed ($^1J_{HPt} = 812$ Hz). The ^{31}P NMR spectrum at room temperature is broad and complex with multiple resonances between −3 and 13 ppm. On warming to 60 °C these resonances sharpen, but no limiting spectrum is reached. At temperatures above 60 °C, irreversible spectral changes occur.

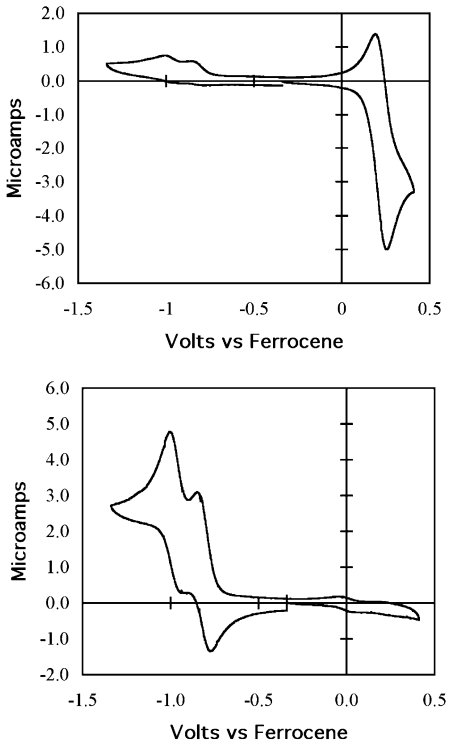

Figure 3. Cyclic voltammograms recorded on [Pt(EtXantphos)$_2$](BF$_4$)$_2$ (1.0×10^{-3} M, bottom trace) and [HPt(EtXantphos)$_2$](PF$_6$) (1.4×10^{-3} M, top trace) in acetonitrile. Conditions: scan rate 50 mV/s, 0.3 M NEt$_4$BF$_4$, glassy carbon electrode.

Electrochemical Studies. Figure 3 shows cyclic voltammograms recorded on [Pt(EtXantphos)$_2$](BF$_4$)$_2$ and [HPt(EtXantphos)$_2$](PF$_6$) in acetonitrile at room temperature (22 ± 1.5 °C). [Pt(EtXantphos)$_2$](BF$_4$)$_2$ has two quasi-reversible, one-electron reductions at −0.81 ($\Delta E_p = 95$ mV) and −0.97 V ($\Delta E_p = 80$ mV) versus ferrocene, as shown in the bottom trace of Figure 3. A linear plot of i_p versus the square root of the scan rate indicates that the electron-transfer reactions are diffusion-controlled. Cyclic voltammograms recorded on Pt(EtXantphos)$_2$ in benzonitrile gave similar results. These data indicate the formation of a stable Pt(I) complex on the time scale of the cyclic voltammetry experiment. In previous studies, it has been shown that diphosphine ligands with large chelate bites can be used to stabilize Pd(I), Ni(I), and Ir(0) complexes with respect to disproportionation reactions.[32−34]

As shown by the top trace in Figure 3, [HPt(EtXantphos)$_2$](PF$_6$) undergoes a quasi-reversible ($\Delta E_p = 60$ mV, $i_{pa}/i_{pc} = 0.8$) one-electron oxidation at +0.23 V versus ferrocene in acetonitrile. This oxidation wave is diffusion-controlled, as indicated by a square-root dependence of the peak current on the scan rate, and the one-electron nature of the wave is supported by the difference in peak potentials of 60 mV compared to a theoretical value of 60 mV. Comparison of the peak

current observed for the oxidation of $[HPt(EtXantphos)_2]^+$ with the peak current for the reduction of $[Pt(EtXantphos)_2]^{2+}$ ($i_{pa}[HPt(EtXantphos)_2]^+/i_{pc}[Pt(EtXantphos)_2]^{2+} = 1.0$) also indicates a one-electron transfer. The observation that the cathodic wave of $[HPt(EtXantphos)_2]^{2+}$ is somewhat smaller than the anodic wave of $[HPt(EtXantphos)_2]^+$ and the appearance of the two reduction waves associated with $[Pt(EtXantphos)_2]^{2+}$ at −0.81 and −0.97 V are consistent with a disproportionation of $[HPt(EtXantphos)_2]^{2+}$ to form $[(H)_2Pt(EtXantphos)_2]^{2+}$ and $[Pt(EtXantphos)_2]^{2+}$ by hydrogen atom transfer. The waves at −0.81 and −0.97 V are associated with $[Pt(EtXantphos)_2]^{2+}$, and they are not observed if the initial scan direction is negative. These waves are observed only after traversing the Pt(II/III) couple of $[HPt(EtXantphos)_2]^+$. Reversible one-electron oxidations followed by disproportionation reactions have also been observed for the isoelectronic $HCo(dppe)_2$ and $HRh(dppe)_2$ complexes (where dppe is bis(diphenylphosphino)ethane).[28,42]

Equilibrium Measurements. The pK_a of $[(H)_2Pt(EtXantphos)_2]^{2+}$ was determined at room temperature (22 ± 1.5 °C) by equilibration of $[HPt(EtXantphos)_2]^+$ with an excess of a mixture of cyanoaniline and cyanoanilinium tetrafluoroborate to fix the solution pH (reaction 2). This reaction comes to equilibrium over a period of approximately 20 min, as indicated by a constant ratio of $[(H)_2Pt(EtXantphos)_2]^{2+}$ to $[HPt(EtXantphos)_2]^+$. The equilibrium constant calculated for this reaction is 0.14 ± 0.03, based on an integration of the hydride region of the ^{1}H NMR spectra for four separate reactions. The ratio of cyanoaniline to cyanoanilinium was determined from the stoichiometry of the reaction and by using a large excess of both cyanoanilinium and cyanoaniline. Addition of pK_2 (−0.8) to the pK_a value of cyanoanilinium tetrafluoroborate (7.6)[37] gives a pK_a value of 6.8 ± 0.5 for $[(H)_2Pt(EtXantphos)_2]^{2+}$. The precision of the measurements indicates an error of less than 0.1 pK_a units. However, there is uncertainty in the temperature (±1.5 °C), and there is also uncertainty in the values of the reference compounds (±0.1 pK_a units). This could lead to further estimated errors of ±0.2 pK_a units. As a result, we have used a conservative error estimate of ±0.5 pK_a units (±0.7 kcal/mol).

$$[HPt(EtXantphos)_2]^+ + [NCC_6H_4NH_3]^+ \leftrightarrow [(H)_2Pt(EtXantphos)_2]^{2+} + NCC_6H_4NH_2 \quad (2)$$

The pK_a of $[HPt(EtXantphos)_2]^+$ was determined by reaction with $Ni(dmpe)_2$ (where dmpe is bis(dimethylphosphino)ethane) to form $Pt(EtXantphos)_2$ and $[HNi(dmpe)_2]^+$ in benzonitrile, as shown in reaction 3. This reaction requires a period of 3−4 h to reach equilibrium. The equilibrium constant for this reaction ($K_3 = (1.0 \pm 0.5) \times 10^{-3}$) was determined by an integration of the ^{31}P NMR spectrum in which all four species can be observed for four separate experiments. The use of benzonitrile was necessary because of the low solubility of the neutral Ni(0) and Pt(0) complexes in acetonitrile. The difference in relative pK_a values measured in these solvents has been shown previously to be small.[24,26]

Scheme 3

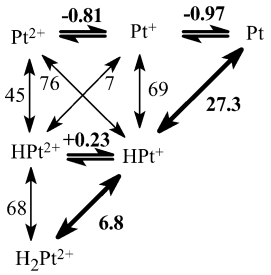

Adding pK_3 to the pK_a of $[HNi(dmpe)_2]^+$ (24.3)[24] gives a pK_a value of 27.3 ± 0.5 for $[HPt(EtXantphos)_2]^+$. As a further check, equilibration of $Pt(EtXantphos)_2$ with $[(Me_2N)_3P{=}NHMe](BF_4)$ (pK_a = 27.5)[36] gave an equilibrium constant of 0.51, which corresponds to a pK_a value of 27.2 for $[HPt(EtXantphos)_2]^+$.

$$[HPt(EtXantphos)_2]^+ + Ni(dmpe)_2 \leftrightarrow Pt(EtXantphos)_2 + [HNi(dmpe)_2]^+ \quad (3)$$

Determination of Solution Bond-Dissociation Free Energies. The thermodynamic relationships between the various metal complexes that comprise the $[(H)_2Pt(Xantphos)_2]^{2+}$ system are illustrated in Scheme 3. For simplicity, the two EtXantphos ligands are not indicated. In Scheme 3, vertical arrows show homolytic bond-dissociation reactions; proton-transfer reactions are represented by diagonal arrows pointing up and to the right; and hydride-transfer reactions are indicated by arrows pointing up and to the left. Reversible arrows between columns indicate one-electron-transfer reactions. Bold numbers and arrows indicate the five experimentally measured values. These values are the potentials associated with the three reversible or quasi-reversible, one-electron-transfer reactions described above and the two pK_a measurements associated with the successive deprotonation of $[(H)_2Pt(EtXantphos)_2]^{2+}$. Normal text indicates values determined using thermodynamic cycles.

Scheme 3 is useful for deriving the thermodynamic cycles that relate various thermodynamic parameters. For example, the homolytic bond-dissociation reaction of $[HPt(EtXantphos)_2]^+$ to form a hydrogen atom and $[Pt(EtXantphos)_2]^+$ can also be achieved by a cycle of three sequential reactions: (1) deprotonation of $[HPt(EtXantphos)_2]^+$ to form $Pt(EtXantphos)_2$, (2) oxidation of $Pt(EtXantphos)_2$ by one electron to form $[Pt(EtXantphos)_2]^+$, and (3) reduction of the proton by one electron to form a hydrogen atom. This sequence of reactions (reactions 4−7) and their associated free energies lead immediately to the relationship shown in eq 8. In eq 8, pK_a is the pK_a of the hydride under consideration, $E_{1/2}(CB/CB^+)$ is the oxidation potential of the conjugate base formed by deprotonation of the hydride, and 53.6 represents the free energy (in kcal/mol) associated with reduction of a proton to a hydrogen atom in acetonitrile.[13,43] A homolytic bond dissociation free energy of 69 ± 2 kcal/mol was determined for $[HPt(EtXantphos)_2]^+$ using eq 8. Equation 8 and the cycle on which it is based have been widely used for determining

(42) (a) Pilloni, G.; Schiavon, G.; Zotti, G.; Zecchin, S. *J. Organomet. Chem.* **1977**, *134*, 305−318. (b) Pilloni, G.; Vecchi, E.; Martelli, M. *Electroanal. Chem Interfac. Electrochem.* **1973**, *45*, 483−487.

(43) Ellis, W. W.; Raebiger, J. W.; Curtis, C. J.; Bruno, J. W.; DuBois, D. L. *J. Am. Chem. Soc.* **2004**, *125*, accepted.

Table 3. Thermodynamic Parameters for [(H)$_2$Pt(EtXantphos)$_2$]$^+$ and Its Derivatives[a]

compound	$E_{1/2}$(CB/CB$^+$)[b]	pK_a	$\Delta G_{H^\bullet}$ (kcal/mol)	ΔG_{H^-} (kcal/mol)
[(H)$_2$Pt(EtXantphos)$_2$]$^{2+}$	+0.23 ± 0.02	6.8 ± 0.5	68 ± 2	
[HPt(EtXantphos)$_2$]$^+$	−0.97 ± 0.02	27.3 ± 0.5	69 ± 2	76 ± 2
[HPt(EtXantphos)$_2$]$^{2+}$	−0.81 ± 0.02	7.1 ± 1.2	45 ± 2	

[a] Uncertainties for all of the values are discussed in the text. All values are for 22 ± 1.5 °C. [b] Half-wave potentials vs ferrocene for oxidation of the conjugate bases of the compounds indicated.

homolytic bond-dissociation free energies (and enthalpies after an entropy correction) for a number of transition metal hydrides.[13−17] Equation 8 was also used to calculate a homolytic bond-dissociation free energy of 68 ± 2 kcal/mol for [(H)$_2$Pt(EtXantphos)$_2$]$^{2+}$ from the pK_a of [(H)$_2$Pt(EtXantphos)$_2$]$^{2+}$ and the oxidation potential of [HPt(EtXantphos)$_2$]$^+$. The uncertainties in these values include the uncertainty associated with the pK_a measurement, ±0.7 kcal/mol as discussed above under equilibrium measurements, and the uncertainty in the electrochemical measurement estimated at ±0.02 V (±0.5 kcal/mol). This gives an estimated error of ±1.2 kcal/mol.

$$\Delta G$$

$$HML_n^+ \rightarrow ML_n + H^+ \quad 1.37pK_a \tag{4}$$

$$ML_n \rightarrow ML_n^+ + e^- \quad 23.06E_{1/2}(CB/CB^+) \tag{5}$$

$$H^+ + e^- \rightarrow H^\bullet \quad 53.6 \tag{6}$$

$$\text{net: } HML_n^+ \rightarrow ML_n^+ + H^\bullet \tag{7}$$

$$\Delta G_{H^\bullet} = 1.37pK_a + 23.06E_{1/2}(CB/CB^+) + 53.6 \tag{8}$$

The free energy associated with heterolytic cleavage of the Pt−H bond of [HPt(EtXantphos)$_2$]$^+$ to form a hydride ion and [Pt(EtXantphos)$_2$]$^{2+}$ can be calculated by a slight modification of this cycle in which the conjugate base of the hydride is oxidized by two electrons and the proton is reduced by two electrons to form a hydride ion. This cycle results in eq 9,[24] which can be used to calculate a hydride donor ability of 76 ± 2 kcal/mol for [HPt(EtXantphos)$_2$]$^+$. Because there are two half-wave potentials with estimated errors of ±0.5 kcal/mol and a pK_a measurement with an estimated error of ±0.7 kcal/mol, the total error is estimated at ±1.7 kcal/mol. A cycle involving the reduction of [HPt(EtXantphos)$_2$]$^{2+}$ to [HPt(EtXantphos)$_2$]$^+$, the homolytic cleavage of the Pt−H bond of [HPt(EtXantphos)$_2$]$^+$, and the oxidation of the hydrogen atom to a proton can be used to calculate a pK_a of 7.1 ± 1.2 for [HPt(EtXantphos)$_2$]$^{2+}$. From this pK_a value and eq 8, a homolytic bond-dissociation energy of 45 ± 2 kcal/mol is determined for [HPt(EtXantphos)$_2$]$^{2+}$. The thermodynamic values of the platinum hydride complexes are summarized in Table 3.

$$\Delta G_{H^-} = 1.37pK_a + 46.1E_{1/2}(CB/CB^{2+}) + 79.6 \tag{9}$$

Discussion

Hydricity of [HPt(EtXantphos)$_2$]$^+$. Only one hydride transfer reaction is present in Scheme 3, the transfer of a hydride from [HPt(EtXantphos)$_2$]$^+$ to form [Pt(EtXantphos)$_2$]$^{2+}$. The hydride donor ability of [HPt(EtXantphos)$_2$]$^+$ is 76 kcal/mol. In comparison, [HPt(dmpe)$_2$]$^+$, [HPt(depe)$_2$]$^+$, and [HPt(dppe)$_2$]$^+$ (where depe is bis(diethylphosphino)ethane and dppe is bis(diphenylphosphino)ethane) have ΔG_{H^-} values of 42, 44, and 52 kcal/mol, respectively.[24,26] Both the electron-withdrawing ability of the xanthene bridge (a substituent effect) and the chelate bite size play a role in the 32 kcal/mol difference between the hydride donor ability of [HPt(EtXantphos)$_2$]$^+$ and [HPt(depe)$_2$]$^+$. The difference in the hydricity observed for [HPt(depe)$_2$]$^+$ and [HPt(dppe)$_2$]$^+$ is 8 kcal/mol for replacing eight phenyl substituents with eight ethyl substituents. In comparing [HPt(EtXantphos)$_2$]$^+$ and [HPt(depe)$_2$]$^+$, two xanthene bridges replace the two ethylene bridges, or four aryl substituents replace four ethylene substituents. As a result, we estimate a substituent effect for these two complexes of approximately 4 kcal/mol. Therefore, the much larger chelate bite of EtXantphos compared to depe is estimated to contribute approximately 28 kcal/mol to the difference in the hydride donor abilities of these two complexes. This large chelate-bite contribution to hydricity is comparable to that observed for analogous palladium complexes.[32] The large chelate bite associated with the EtXantphos ligand results in a significant tetrahedral distortion from a square-planar geometry for [M(diphosphine)$_2$]$^{2+}$ complexes (M = Ni, Pd, Pt). This distortion stabilizes the lowest unoccupied molecular orbital (LUMO), the d(x^2-y^2) orbital in ligand field theory. The lower energy of the LUMO makes [M(diphosphine)$_2$]$^{2+}$ complexes with large bite angles and large tetrahedral distortions better hydride acceptors than analogous complexes with small bite sizes.[24,30,32]

HPt(EtXantphos)$_2$]$^+$ is a poorer hydride donor by 6 kcal/mol than [HPd(EtXantphos)$_2$]$^+$ (70 kcal/mol).[32] This agrees with the hydride donor abilities increasing in the order first row ≪ third row < second row for five-coordinate 18-electron hydrides.[29,44] In fact, HPt(EtXantphos)$_2$]$^+$ is the poorest hydride donor of any transition metal hydride studied to date for which an accurate thermodynamic measurement has been made.[24−26,28−32,43,44] From the opposite perspective, [Pt(EtXantphos)$_2$]$^{2+}$ is an excellent hydride acceptor. HPt(EtXantphos)$_2$]$^+$ is a 42 kcal/mol poorer hydride donor than HRh(dppb)$_2$ (ΔG_{H^-} = 34 kcal/mol)[29] and a 40 kcal/mol poorer hydride donor than [HW(CO)$_4$PPh$_3$]$^-$ (ΔG_{H^-} = 36 kcal/mol).[31] It is likely that this range can be significantly extended on both ends of this scale for the [HM(diphosphine)$_2$]$^+$ (M = Ni, Pd, and Pt) and HM(diphosphine)$_2$ complexes (M = Co, Rh, and Ir). As a result, this class of compounds is a very interesting one for probing the effects of hydride donor abilities on various reactions.

Acidity of Platinum Hydrides. The pK_a of [HPt(EtXantphos)$_2$]$^+$ is 27.2. This value is less than that of [HPt(depe)$_2$]$^+$ (29.7) and larger than [HPt(dppe)$_2$]$^+$ (22.0).[24,26] The difference in pK_a values for the latter two

(44) Curtis, C. J.; Miedaner, A.; Raebiger, J. W.; DuBois, D. L. *Orgnometallics*, **2004**, *23*, 511−516.

complexes suggests a correction factor of approximately 1 pK_a unit whenever an ethyl group is substituted for a phenyl group. Substitution of an ethylene bridge by an aryl bridge would therefore be expected to result in a decrease in the pK_a of a complex by 2 units for each bridge. Thus a pK_a slightly larger than 26 is anticipated for $[HPt(EtXantphos)_2]^+$ on the basis of electronic effects associated with replacing the CH_2CH_2 bridge with xanthene, which is slightly more electron-donating than a phenyl substituent because of the ortho oxygen. Unlike hydricity, which exhibits large bite size effects for $[HM(diphosphine)_2]^+$ complexes, the acidity does not appear to be influenced to any significant extent by this parameter.[24,30,32] $[HPt(EtXantphos)_2]^+$ is less acidic than $[HPd(EtXantphos)_2]^+$ (pK_a = 18.5),[32] consistent with an increasing acidity order of third row ≪ first row < second row for this class of complexes.[29,44]

From the hydricity of $[HPt(EtXantphos)_2]^+$, an acid with a pK_a value of 0 or less in acetonitrile is required for hydrogen evolution to become favorable. This is based on a value of 76 kcal/mol for the heterolytic cleavage of hydrogen in acetonitrile.[13,26,30] However, protonation of $[HPt(EtXantphos)_2]^+$ to form the dihydride should occur for acids with pK_a values of 6.8 or less in acetonitrile. As a result, instead of observing hydrogen loss, a stable dihydride is formed when excess triflic acid or tetrafluoroboric acid is reacted with $[HPt(EtXantphos)_2]^+$ in acetonitrile or benzonitrile. This dihydride is a strong acid. On an aqueous scale, $[(H)_2Pt(EtXantphos)_2]^{2+}$ would have a pK_a of approximately −1, because pK_a values measured in acetonitrile are approximately 7.5 units larger than the corresponding pK_a values in water.[1] For comparison, $HCo(CO)_4$ is considered a strong organometallic acid with a pK_a in acetonitrile of 8.4.[3]

Oxidation of $[HPt(EtXantphos)_2]^+$ to form $[HPt(EtXantphos)_2]^{2+}$ occurs reversibly with an increase in acidity from 27 to 7 pK_a units. The acidity of $[HPt(EtXantphos)_2]^{2+}$ is the same as that of $[(H)_2Pt(EtXantphos)_2]^{2+}$; as a result, $[HPt(EtXantphos)_2]^{2+}$ can protonate $[HPt(EtXantphos)_2]^+$ to form $[(H)_2Pt(EtXantphos)_2]^{2+}$ and $[Pt(EtXantphos)_2]^+$. The driving force for this reaction is low, and as a result, the rate of this reaction is expected to be slow. This feature probably contributes to the reversibility of the oxidation of $[HPt(EtXantphos)_2]^+$. However, $[HPt(EtXantphos)_2]^{2+}$ is unstable with respect to a disproportionation reaction involving hydrogen atom transfer as discussed next.

Homolytic Bond-Dissociation Free Energies. The homolytic bond dissociation free energy of $[HPt(EtXantphos)_2]^+$ is 69 kcal/mol in acetonitrile. This value is larger than that observed for $[HPd(diphosphine)_2]^+$ and $[HNi(diphosphine)_2]^+$ complexes, which have homolytic bond-dissociation free energies of 57 ± 2 and 53−56 kcal/mol, respectively.[24,30,32] For the nickel and palladium complexes, the homolytic BDFEs have been found to be only slightly dependent on substituent effects and independent of chelate bite size. It is anticipated that this will be true for platinum as well. The dependence of the homolytic BDFEs for these $[HM(diphosphine)_2]^+$ complexes (where M = Ni, Pd, and Pt) is therefore third row > second row > first row. In general, previous studies of homolytic bond cleavage reactions have reported enthalpy values and not free-energy values. To convert from free-energy values to enthalpy values, it has been suggested that 4.8 kcal/mol be added to the free-energy values measured in acetonitrile.[13] This results in a homolytic bond-dissociation enthalpy of 74 kcal/mol for $[HPt(EtXantphos)_2]^+$. This agrees well with the homolytic bond-dissociation energy of *trans*-$HPt(PPh_3)_2Cl$ (73 kcal/mol),[45] and it is comparable to the homolytic bond-dissociation energies of other second- and third-row transition metals, e.g., $HMo(CO)_3Cp$ (70 kcal/mol), $HW(CO)_3Cp$ (73 kcal/mol), and $HRe(CO)_5$ (75 kcal/mol).[14] An unusual feature of $[HPt(EtXantphos)_2]^+$ is that the radical produced by bond cleavage, $[Pt(EtXantphos)_2]^+$, is stable, as indicated by two reversible electron-transfer reactions for the Pd(II/I) and Pd(I/0) couples. $[Pt(EtXantphos)_2]^+$ does not undergo rapid dimerization, as has been observed for most 17-electron radicals. Further study of the reactivity of $[Pt(EtXantphos)_2]^+$ is clearly warranted, but it is beyond the scope of the present work.

The homolytic bond-dissociation free energy of $[(H)_2Pt(EtXantphos)_2]^{2+}$ (68 kcal/mol) is the same within experimental error as that measured for $[HPt(EtXantphos)_2]^+$ (69 kcal/mol). However, it is significantly larger than the homolytic bond-dissociation free energy of $[HPt(EtXantphos)_2]^{2+}$ (45 kcal/mol). This indicates that $[HPt(EtXantphos)_2]^{2+}$ is unstable, by 23 kcal/mol, with respect to disproportionation to form $[Pt(EtXantphos)_2]^{2+}$ and $[(H)_2Pt(EtXantphos)_2]^{2+}$. This situation is similar to that observed for $[HRh(dppe)_2]^+$ and $[HCo(dppe)_2]^+$, which are known to undergo disproportionation reactions.[42] The sum of the two successive homolytic bond-dissociation free energies of $[(H)_2Pt(EtXantphos)_2]^{2+}$ (113 kcal/mol) exceeds the homolytic bond-dissociation free energy of hydrogen in acetonitrile (103.6 kcal/mol).[13] This is consistent with the observed oxidative addition of H_2 to $[Pt(EtXantphos)_2]^{2+}$ to form $[(H)_2Pt(EtXantphos)_2]^{2+}$ (see Experimental Section).

For square-planar d^8 metal complexes, the thermodynamic driving force for oxidative addition reactions depends on both the metal and chelate bite size. For example, the enthalpy for the oxidative addition of tetrachloro-*o*-benzoquinone to $[M(dppv)_2]^+$ (where dppv is 1,2-bis(diphenylphosphino)ethene) follows the order Co > Ir > Rh.[46] Interestingly, this ordering parallels the hydride acceptor ability of bis(diphosphine) complexes of Ni, Pd, and Pt. As discussed above, $[Pt(EtXantphos)_2]^{2+}$ reacts with hydrogen to form a dihydride, whereas $[Pt(diphosphine)_2]^{2+}$ complexes with smaller chelate bite sizes do not. The dependence of these oxidative-addition reactions on metal and chelate bite size suggests that LUMO energies control oxidative addition reactions as well as the hydride acceptor abilities for these 16-electron bis(diphosphine) complexes.

As shown in Scheme 3, oxidative addition of hydrogen to square-planar d^8 transition metal complexes can be regarded as the sequential addition of hydrogen atoms to form the dihydride. The first addition of a hydrogen atom, however, is very similar to electrochemical reduction from a 16-electron to a 17-electron complex, which is dependent on the chelate bite size. Therefore the

(45) Mortimer, C. T. *Rev. Inorg. Chem.* **1984**, *6*, 233.
(46) Mondal, J. U.; Bulls, R.; Blake, D. M. *Inorg. Chem.* **1982**, *21*, 1668−1670.

homolytic bond-dissociation free energy of this 17-electron complex should depend on chelate bite size. It is this homolytic bond-dissociation free energy that produces the observed dependence on chelate bite size for the oxidative addition of hydrogen.

Summary

The reduction of Pt(COD)Cl$_2$ (where COD is 1,4-cyclooctadiene) with hydrazine in the presence of 2 equiv of EtXantphos results in the formation of [HPt(EtXantphos)$_2$]$^+$. This hydride can be reversibly protonated, deprotonated, and oxidized. The combination of the thermodynamic data associated with these transformations and the Pt(I/0) and Pt(II/I) potentials of Pt(EtXantphos)$_2$ leads to a fairly complete thermodynamic characterization of the Pt−H bonds of [HPt(EtXantphos)$_2$]$^+$, [HPt(EtXantphos)$_2$]$^{2+}$, and [(H)$_2$Pt(EtXantphos)$_2$]$^{2+}$. For square-planar 16-electron complexes, the free energies associated with the addition of molecular hydrogen, hydrogen atoms, hydride ions, and electrons are all expected to increase (become more positive) as the chelate bite size decreases, because the energy of the LUMO increases. The hydride donor ability of [HPt(EtXantphos)$_2$]$^+$ and [HPt(depe)$_2$]$^+$ differs by 32 kcal/mol, of which 28 kcal/mol is estimated to arise from chelate bite size effects. This large contribution of the bite size to hydride donor abilities indicates that the chelate bite size is very useful in controlling the thermodynamic hydride donor abilities of five-coordinate, 18-electron complexes independent of the acidity of these complexes, which is not effected by chelate bite size. HPt(EtXantphos)$_2$]$^+$ is a 42 kcal/mol poorer hydride donor than HRh(dppb)$_2$; as a result, this isostructural and isoelectronic class of compounds is a very interesting one for probing the effects of hydride donor abilities on various reactions.

Acknowledgment. The support of the U.S. Department of Energy, Office of Science, Chemical and Biological Sciences Division, under DOE contract No. DE-AC36-99GO10337 is gratefully acknowledged.

Supporting Information Available: Tables of crystal data, data collection parameters, structure solution and refinement, atomic coordinates and equivalent isotropic displacement parameters, bond lengths, bond angles, anisotropic thermal parameters, hydrogen coordinates, and isotropic displacement parameters for Pt(EtXantphos)$_2$. This information is available free of charge via the Internet at http://pubs.acs.org.

OM034238I